Koch, S. A., Fikar, R., Millar, M. & O'Sullivan, T. (1984). *Inorg. Chem.* **23**, 121–122.
Morpurgo, G. O., Dessy, G. & Fares, V. (1984). *J. Chem. Soc. Dalton Trans.* pp. 785–791.

Reibenspies, J. H., Anderson, O. P., Laird, S. K. & Brito, K. K. (1983). *Proc. Am. Crystallogr. Assoc. Meet.*, Abstr. p. 49.
Sheldrick, G. M. (1983). *SHELXTL Users Manual.* Revision 4. Nicolet XRD Corporation, Madison, Wisconsin, USA.

Structures of Four- and Five-Carbon Alkyldiammonium Tetrachlorocuprate(II) and Tetrabromocuprate(II) Salts

By John K. Garland

Department of Chemistry, Washington State University, Pullman, WA 99164-4630, USA

Kenneth Emerson

Department of Chemistry, Montana State University, Bozeman, MT 59717, USA

and Mark R. Pressprich

Department of Chemistry, Washington State University, Pullman, WA 99164-4630, USA

Abstract. 1,4-Butanediammonium tetrabromocuprate(II), $C_4H_{14}N_2^{2+}.CuBr_4^{2-}$, $M_r = 473$, monoclinic, $P2_1/a$, $a = 7.914$ (2), $b = 7.887$ (4), $c = 9.432$ (2) Å, $\beta = 102.83$ (2)°, $V = 574$ Å^3, $Z = 2$, $D_x = 2.74$ g cm^{-3}, $\lambda(Mo\ K\alpha) = 0.71069$ Å, $\mu = 157$ cm^{-1}, $T = 293$ K, $F(000) = 442$, 1259 unique reflections, of which 1192 with $F \geq 3\sigma(F)$ were refined to a final $R = 0.0439$ for the 3σ data set with empirical extinction corrections ($wR = 0.0541$). The following structures used reflections with $F \geq 6\sigma(F)$. 1,4-Butanediammonium tetrachlorocuprate(II), $C_4H_{14}N_2^{2+}.CuCl_4^{2-}$, $M_r = 296$, monoclinic, $P2_1/a$, $a = 7.588$ (1), $b = 7.599$ (1), $c = 9.268$ (1) Å, $\beta = 103.14$ (1)°, $V = 520$ Å^3, $Z = 2$, $D_x = 1.88$ g cm^{-3}, Mo $K\alpha$, $\mu = 31.7$ cm^{-1}, $F(000) = 298$, 1184 unique reflections, 786 of 805 for the 6σ data set after discarding twin overlaps were refined to a final $R = 0.0652$ ($wR = 0.0861$). 1,5-Pentanediammonium tetrabromocuprate(II), $C_5H_{16}N_2^{2+}.CuBr_4^{2-}$, $M_r = 487$, monoclinic, $P2_1/n$, $a = 8.142$ (3), $b = 7.560$ (2), $c = 21.736$ (10) Å, $\beta = 101.49$ (3)°, $V = 1311$ Å^3, $Z = 4$, $D_x = 2.47$ g cm^{-3}, Mo $K\alpha$, $\mu = 146$ cm^{-1}, $F(000) = 916$, 3527 unique reflections, 995 of 1030 for the 6σ data set were refined to a final $R = 0.0734$ ($wR = 0.0948$). 1,5-Pentanediammonium tetrachlorocuprate(II), $C_5H_{16}N_2^{2+}.CuCl_4^{2-}$, $M_r = 308$, monoclinic, $P2_1/n$, $a = 7.747$ (3), $b = 7.203$ (2), $c = 21.761$ (6) Å, $\beta = 102.12$ (2)°, $V = 1188$ Å^3, $Z = 4$, $D_x = 1.73$ g cm^{-3}, Mo $K\alpha$, $\mu = 27.5$ cm^{-1}, $F(000) = 628$, 2842 unique reflections, 501 of 530 for the 6σ data set were refined to a final $R = 0.0925$ ($wR = 0.1096$). Each Cu^{II} ion has two short and two long (semi-coordinate) bonds to halide ions forming sheets puckered from the *ab* plane plus two short bonds to halide ions axial to the sheets, completing a tetragonally elongated octahedral coordination. Adjacent sheets have axial halide ions in an eclipsed conformation. The diammonium ions provide links between sheets, hydrogen bonding to the halides. The C_4 salts have the two ends of the diammonium ions equivalent by symmetry with C_4 chains *trans* around the central bond and *gauche* for N *versus* C positioning around each terminal C—C bond. The hydrogen bonds include one to an axial halide, arranged *gauche* to the N—C—C alignment, and two to sheet halides, one *gauche* and one *trans* to the N—C—C alignment. The C_5 chains are *trans* at both of the C—C—C—C sites, one N—C—C—C site is *trans* and one *gauche*, and both N atoms have two hydrogen bonds to axial halides and one to a sheet halide. The C_5 chains have about a 90° different direction of approach at the two ends.

Introduction. The monoammonium alkylammonium salts of copper(II) tetrahalides, $(C_nH_{2n+1}NH_3)_2CuX_4$, form puckered antiferrodistortive layer perovskite structures with adjacent layers staggered which give strong ferromagnetic interactions in the copper-halogen sheet layer and weak magnetic interactions between layers (Willett, 1964; Steadman & Willett, 1970; Barendrecht & Shenk, 1970; de Jongh & van Amstel, 1971; de Jongh, van Amstel & Miedema, 1972; Drumheller, Dickey, Reckliss, Zaspel & Glass, 1972; Zaspel & Drumheller, 1977; Wong, Willett & Drumheller, 1981). The structures contain layers of square-planar CuX_4^{2-} anions. In each anion, two Cu—X bonds are involved in bridges to adjacent

© 1990 International Union of Crystallography

anions while the other two Cu—X bonds are nearly normal to the layer. The alkyldiammonium (ADA) series, $(H_3NC_nH_{2n}NH_3)CuX_4$, form structures with eclipsed adjacent layers (Anderson & Willett, 1971; Birrel & Zaslow, 1972; Phelps, Losee, Hatfield & Hodgson, 1976; Tichy, Benes, Haelg & Arend, 1978; Halvorson & Willett, 1988). These eclipsed structures have bonds on adjacent layers nearly directly over each other and show much stronger interlayer magnetic interactions, presumably *via* superexchange through a two-halide bridge (Phelps, Losee, Hatfield & Hodgson, 1976; Von Kanel, 1979; Snively, Seifurt, Emerson & Drumheller, 1979; Snively, Drumheller & Emerson, 1981; Snively, Tuthill & Drumheller, 1981; Snively, Haines, Emerson & Drumheller, 1982; Rubenacker, Haines, Drumheller & Emerson, 1984; Halvorson & Willett, 1988; Middleton, Place & Willett, 1988).

As chain length grows, monoclinic units of $(ADA)CuX_4$, nD–X, structures deviate more from linear two-halide bridging with an increase in the halide–halide interlayer separation. The 1,4-butanediammonium salt $4D$–Cl has about the same interlayer distance as the 1,3-propanediammonium salt $3D$–Cl (Snively, Drumheller & Emerson, 1981). The extra chain length is accommodated by the monoclinic angle and coiling of the chains. This work presents the crystal structures of $4D$–Cl, $4D$–Br and of the 1,5-pentanediammonium compounds, $5D$–Br and $5D$–Cl. The $5D$ members of the series are interesting because $5D$–Br has an interlayer exchange which cannot be clearly interpreted as ferromagnetic or antiferromagnetic (Rubenacker, Haines, Drumheller & Emerson, 1984). The interlayer exchange is antiferromagnetic for $n = 2$ to 9 in the nD–Cl series and for $n = 2, 3, 4, 6, 8$ in the nD–Br series. $7D$–Br, $9D$–Br, $10D$–Br, and $10D$–Cl have ferromagnetic interlayer coupling. The interlayer exchange becomes much weaker as the ADA chains lengthen, as expected if the two-halide superexchange decreases when the separation increases. Our data, earlier diffractometer data (Phelps, Losee, Hatfield & Hodgson, 1976; Tichy, Benes, Haelg & Arend, 1978) and diffractometer data on $2D$–Br and $3D$–Br are used to discuss correlation between magnetic data and the overlap between axial halides from adjoining layers (Halvorson & Willett, 1988).

Experimental. $4D$–Cl, $4D$–Br, $5D$–Cl and $5D$–Br were formed by reaction in water of approximately equimolar amounts of the diamine and CuX_2 and slightly over twice that many moles of HX. Crystals were formed by slow evaporation of water from the orginal mixture or from redissolved portions.

$4D$–Cl and $5D$–Cl crystals were examined under a polarizing microscope and selected for good extinctions upon rotation. The opaque $4D$–Br and $5D$–Br were examined under a binocular microscope and selected for smoothness of faces. Weissenberg or precession photography was used to eliminate poor Br compound crystals, and other crystals which exhibited excessive twinning were eliminated after preliminary measurements on the diffractometer.

X-ray diffraction data were collected on a Nicolet $R3m/E$ automated diffractometer. Data were processed on the Data General Eclipse computers of the Nicolet systems at Montana State University and at Washington State University. Crystal sizes: $0.67 \times 0.04 \times 0.88$ mm for $4D$–Br; record lost for $4D$–Cl; $0.30 \times 0.15 \times 0.10$ mm for $5D$–Br; $0.38 \times 0.16 \times 0.01$ mm for $5D$–Cl.

The monoclinic cells and orientation matrices were defined by least-squares refinements of 25 reflections in 2θ ranges 25–35° $4D$–Br, 25–30° $4D$–Cl, 8–30° $5D$–Br and 7–30° $5D$–Cl. $\lambda = 0.71069$ Å. Data were collected for $h \geq 0$ $k \geq 0$ and all l to maximum h, k and l values of 10, 10, 12 ($4D$–Br), 9, 9, 12 ($4D$–Cl), 11, 11, 31 ($5D$–Br), and 11, 11, 31 ($5D$–Cl). Absorption corrections were calculated empirically for laminar sheets with a 3° minimum glancing angle (minimum and maximum transmissions: $4D$–Br, 0.056 and 0.595; $4D$–Cl, 0.493 and 0.970; $5D$–Br, 0.287 and 0.971; $5D$–Cl, 0.628 and 0.930). Three standards were monitored every 100 reflections with variations within counting statistics. Scan speeds ranged from 14.65 to 58.59° min^{-1}. $4D$–Br had 1761 total reflections with $2\theta < 55°$, 1259 unique reflections with 1192 having $F \geq 3\sigma(F)$. $4D$–Cl had 1602 total reflections with $2\theta < 55°$, 1184 unique reflections with 805 having $F \geq 6\sigma(F)$, of which 786 were kept after discarding apparent twin overlaps. $5D$–Br had 4440 total reflections with $2\theta < 60°$, 3527 unique reflections with 1030 having $F \geq 6\sigma(F)$, of which 995 were kept after discarding apparent twin overlaps. $5D$–Cl had 4054 total reflections with $2\theta < 60°$, 2842 unique reflections with 530 having $F \geq 6\sigma(F)$, of which 501 were kept after discarding apparent twin overlaps. Agreement between equivalent reflections: $4D$–Br, $R = 0.0253$; $4D$–Cl, $R = 0.0719$; $5D$–Br, $R = 0.0200$; $5D$–Cl, $R = 0.0157$.

Heavy-atom positions for the four structures were found by Patterson mapping. The C and N atoms were found on difference Fourier maps and included in the calculations. The Cu and halide atoms were refined on F with anisotropic thermal parameters, and H atoms were fixed riding on C or N at calculated positions ($r_{C-H} = r_{N-H} = 0.96$ Å) with isotropic thermal parameters approximately 20% larger than for the corresponding C or N atoms. $4D$–Cl, $5D$–Cl and $5D$–Br had twinning contributions and appear to have some reflections overlapped. Twinned crystals with mirror-image monoclinic cells are a recurring problem with nD–X compounds. The reported $2D$–Cl structure (Tichy, Benes, Haelg & Arend,

Table 1. X-ray data-collection parameters

	4D–Br	4D–Cl	5D–Br	5D–Cl
Omitting below F =	$3\sigma(F)$	$6\sigma(F)$	$6\sigma(F)$	$6\sigma(F)$
Observed reflections	1192	805	1030	530
Discarded apparent overlaps	0	19	35	29
Reflections used	1192	786	995	501
Extinction correction	Yes	No	No	No
R	0·0439	0·0652	0·0734	0·0925
wR	0·0541	0·0861	0·0948	0·1096
Av. Δ/σ	0·094	0·000	0·037	0·037
g	0·0020	0·0010	0·0080	0·00239
Goodness of fit	1·021	1·940	0·898	1·452
Largest residual (e Å⁻³)	1·78	0·68	1·30	1·14
Found near	Cu	Cu	Br(1)	Cu(2)

$R = \sum(|F_o| - |F_c|)/\sum|F_o|$. $wR = [\sum w(|F_o| - |F_c|)^2/\sum w|F_o|^2]^{1/2}$ with $w = 1/[\sigma^2(F_o) + g|F_o|^2]$. $\Delta =$ parameter shift on last cycle and $\sigma =$ e.s.d. in that parameter (SHELXTL; Sheldrick, 1984).

1978) is based on a twinned crystal. We resolved both monoclinic mirror cells with a shared indentical *ab* plane from one 5D–Cl crystal while searching for a less evenly divided crystal. We omitted reflections with $I < 3\sigma(I)$. That avoided some small peaks subject to large errors in case of overlap but left indications of remaining overlaps. High values of Δ/σ, where $\Delta = (|F_o| - |F_c|)$, identify those reflections with poor fit to the refined structure. Random errors should give as many reflections with $|F_o| < |F_c|$ as with $|F_o| > |F_c|$, but we found $|F_o| > |F_c|$ for all of the largest Δ/σ reflections on each of the three compounds with twinning.

Refinements of anisotropic thermal parameters with data sets including those large Δ/σ reflections led to non-positive-definite thermal parameters for some C and N atoms of the ADA chains and gave best R values of just under 10% for 5D–Br, 11·25% for 5D–Cl, and 8·15% for 4D–Cl. For each of these three compounds we then found the largest Δ/σ value for any reflection with $|F_o| < |F_c|$ and eliminated all reflections with even larger Δ/σ. Structure factors taken from SHELXTL (Sheldrick, 1984). Table 1 summarizes the resulting refinements, 5D–Cl still gave some non-positive-definite thermal parameters for anisotropic solutions, so the C and N parameters were left isotropic for 5D–Cl and made anisotropic for 5D–Br and 4D–Cl. Data from these solutions are given in Tables 2 and 3.* Distances and angles for the longer Cu—X bonds were found after the structure refinement and appear in Table 3 without calculated standard deviations.

Discussion. The *nD–X* compounds have copper halide layers with Cu atoms at the corners of a

* Lists of structure factors, anisotropic thermal parameters, and hydrogen-bonding discussion and parameters have been deposited with the British Library Document Supply Centre as Supplementary Publication No. SUP 52792 (34 pp.). Copies may be obtained through The Technical Editor, International Union of Crystallography, 5 Abbey Square, Chester CH1 2HU, England.

Table 2. Atomic coordinates (× 10⁴) and equivalent isotropic thermal parameters (Å² × 10³)

U_{eq} is defined as one third of the trace of the orthogonalized U_{ij} tensor.

	x	y	z	U_{eq}
4D–Cl				
Cu(1)	0	0	0	30 (1)
Cl(1)	2309 (3)	2041 (3)	336 (2)	37 (1)
Cl(2)	536 (3)	−433 (3)	2496 (2)	40 (1)
N(0)	−675 (10)	4634 (9)	7759 (8)	39 (2)
C(1)	−1481 (11)	5616 (14)	6378 (10)	44 (3)
4D–Br				
Cu	0	0	0	24 (1)
Br(1)	2332 (1)	2090 (1)	351 (1)	28 (1)
Br(2)	522 (1)	−428 (1)	2613 (1)	31 (1)
N(0)	4317 (7)	323 (5)	−2297 (5)	34 (2)
C(1)	3563 (8)	−621 (7)	−3663 (6)	34 (2)
C(2)	4828 (7)	−814 (6)	−4630 (6)	29 (2)
5D–Cl				
Cu(1)	0	0	0	34 (2)
Cu(2)	5000	5000	0	29 (2)
Cl(1)	1095 (11)	−289 (12)	1062 (3)	33 (3)
Cl(2)	5191 (11)	4825 (14)	1070 (3)	37 (3)
Cl(3)	1990 (11)	7823 (13)	−164 (4)	39 (3)
Cl(4)	7152 (1)	7266 (15)	140 (3)	40 (3)
N(0)	5343 (37)	238 (43)	987 (11)	37 (6)
C(1)	6767 (47)	−289 (55)	1577 (13)	44 (8)
C(2)	6458 (52)	559 (61)	2160 (17)	54 (10)
C(3)	5009 (63)	−194 (88)	2387 (18)	84 (14)
C(4)	5125 (78)	459 (89)	3099 (23)	93 (16)
C(5)	3693 (78)	−265 (87)	3373 (24)	96 (17)
N(6)	4061 (30)	277 (37)	4012 (9)	24 (5)
5D–Br				
Cu(1)	0	0	0	35 (2)
Cu(2)	5000	5000	0	35 (1)
Br(1)	1102 (3)	−215 (4)	1132 (1)	47 (1)
Br(2)	5175 (3)	4888 (4)	1134 (1)	46 (1)
Br(3)	2010 (3)	7776 (4)	−175 (2)	42 (1)
Br(4)	7179 (3)	7247 (4)	150 (1)	42 (1)
N(0)	5298 (24)	55 (36)	1033 (10)	49 (9)
C(1)	6651 (38)	−245 (49)	1569 (14)	60 (12)
C(2)	6470 (60)	492 (61)	2189 (22)	105 (22)
C(3)	5036 (50)	−78 (102)	2399 (17)	145 (31)
C(4)	5259 (51)	94 (86)	3144 (29)	146 (33)
C(5)	3877 (53)	−408 (46)	3362 (13)	82 (16)
N(6)	4018 (27)	136 (31)	4001 (12)	48 (9)

rectangle with another Cu atom in the center of the rectangle. Halogen atoms near the diagonals have a short bond to one Cu (which has another short bond to a halogen 180° from the first one) and a longer semi-coordinate bond to the Cu at the other end of that diagonal. These 'layer' halogens are puckered above or below the Cu-atom plane. Each Cu also has two 'axial' halogen atoms with short bonds nearly perpendicular to the Cu-atom plane. The Cu-atom plane contains the unique axis of the monoclinic structures found for *nD–X* compounds and has been designated the *ab* plane in all structures reported here. The ADA chains lie close to the *c*-axis direction and link adjoining copper halide layers. Eclipsed structures, where Cu atoms in adjacent layers lie directly above each other have been reported (Phelps, Losee, Hatfield & Hodgson, 1976; Tichy,

Table 3. Bond lengths (Å) and bond angles (°)

4D–Cl

Cu(1)—Cl(1)	2·308 (2)	Cu(1)—Cl(2)	2·280 (2)
Cu(1)—C(2)	1·517 (14)	C(1)—N(0)	1·488 (11)
C(2)—C(2a)	1·484 (18)	Cu(1)—Cl(1a)	3·100 (2)

4D–Br

Cu—Br(1)	2·442 (1)	Cu—Br(2)	2·431 (1)
N(0)—C(1)	1·494 (7)	C(1)—C(2)	1·504 (9)
C(2)—C(2a)	1·515 (11)	Cu—Br(1a)	3·185 (1)

5D–Cl

Cu(2)—Cl(2)	2·307 (6)	Cu(2)—Cl(4)	2·307 (10)
Cu(2)—Cl(3)	3·058 (7)	Cu(1)—Cl(4)	3·020 (10)
Cu(1)—Cl(1)	2·299 (7)	Cu(1)—Cl(3)	2·279 (9)
N(0)—C(1)	1·597 (38)	N(6)—C(5)	1·414 (55)
C(2)—C(3)	1·425 (68)	C(1)—C(2)	1·474 (52)
C(4)—C(5)	1·462 (89)	C(3)—C(4)	1·605 (68)

5D–Br

Cu(1)—Br(1)	2·450 (3)	Cu(1)—Br(3)	2·429 (3)
Cu(1)—Br(4a)	3·164 (3)	Cu(2)—Br(3a)	3·179 (3)
Cu(2)—Br(2)	2·442 (3)	Cu(2)—Br(4)	2·430 (3)
N(0)—C(1)	1·454 (33)	N(6)—C(5)	1·432 (39)
C(2)—C(3)	1·405 (70)	C(1)—C(2)	1·492 (60)
C(4)—C(5)	1·359 (68)	C(3)—C(4)	1·597 (73)

4D–Cl

Cl(1)—Cu(1)—Cl(2)	90·3 (1)	Cl(1)—Cu(1)—Cl(2a)	89·7 (1)
Cl(2)—Cu(1)—Cl(1a)	89·7 (1)	C(2)—C(1)—N(0)	113·2 (7)
C(1)—C(2)—C(2a)	113·9 (10)	Cu(1)—Cl(1)—Cu(1a)	166·2 (1)

4D–Br

Br(1)—Cu—Br(2)	90·2 (1)	Br(1)—Cu—Br(2a)	89·8 (1)
Br(2)—Cu—Br(1a)	89·8 (1)	C(1)—C(2)—C(2a)	113·9 (6)
N(0)—C(1)—C(2)	112·4 (5)	Cu—Br—Cu(2)	166·3 (1)

5D–Cl

Cl(2)—Cu(2)—Cl(4)	90·8 (3)	Cl(1)—Cu(1)—Cl(3)	88·6 (3)
Cl(4)—Cu(2)—Cl(2a)	89·2 (3)	Cl(3)—Cu(1)—Cl(1a)	91·4 (3)
C(1)—C(2)—C(3)	115·0 (37)	Cl(3)—Cu(1)—Cl(3a)	180·0 (1)
C(3)—C(4)—C(5)	113·4 (46)	N(0)—C(1)—C(2)	111·6 (30)
Cu(1)—Cl(3)—Cu(2)	164·5 (3)	C(2)—C(3)—C(4)	109·5 (41)
Cu(2)—Cl(4)—Cu(1)	166·1 (3)	N(6)—C(5)—C(4)	106·8 (42)

5D–Br

Br(1)—Cu(1)—Br(3)	89·3 (1)	Br(2)—Cu(2)—Br(4)	89·7 (1)
Br(3)—Cu(1)—Br(1a)	90·7 (1)	Br(4)—Cu(2)—Br(2a)	90·3 (1)
C(1)—C(2)—C(3)	114·7 (39)	Br(4)—Cu(2)—Br(4a)	180·0 (1)
C(3)—C(4)—C(5)	113·3 (37)	N(0)—C(1)—C(2)	118·0 (30)
Cu(1)—Br(3)—Cu(2)	164·2 (1)	C(2)—C(3)—C(4)	111·8 (36)
Cu(2)—Br(4)—Cu(1)	166·3 (1)	N(6)—C(5)—C(4)	110·3 (35)

Benes, Haelg & Arend, 1978; Halvorson & Willett, 1988). Fig. 1 shows the Cu and Br atoms only of our 4D–Br structure with solid lines for the short Cu—Br bonds and dashed lines for the long Cu—Br bonds.

Table 4 summarizes the nD–X structures for n = 2 to 5 and X = Br or Cl with earlier structures transformed as needed to put the copper halide layers in the ab plane. Earlier data from Weissenberg or precession photographs are similar to the diffractometer results shown for 2D–Br, 2D–Cl, 3D–Cl, and 4D–Cl. The orthorhombic crystal for 3D–Cl is the only exception to the eclipsed monoclinic pattern. The longer diammonium ion chain length plus the amount of deviation of β from 90° brings the layers in 5D–Br and 5D–Cl to about halfway between the eclipsed and staggered forms. The P2₁/n cell choice shows 5D–Br, 5D–Cl and 3D–Br as eclipsed layers and corresponds to stacking two P2₁/a units similar to other nD–X compounds. The layer separations along the perpendicular to the layers and single-layer separation ($\frac{1}{2}$ of cell) units for 3DA and 5DA compounds are shown to simplify direct comparisons.
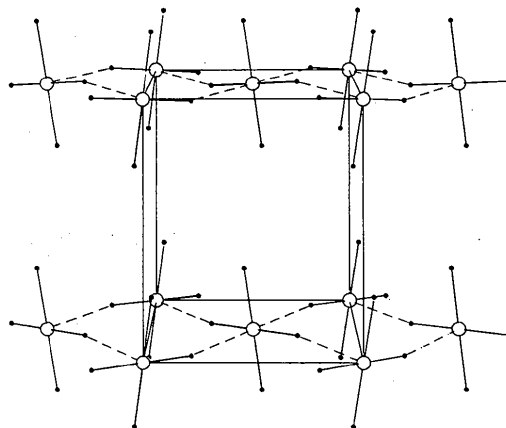

Fig. 1. Cu- and Br-atom positions and linkages in 4D–Br.

Table 4. Lattice parameters, eclipsed layer cells (chosen so layer is in ab plane)

	Space group	a (Å)	b (Å)	c (Å)	β (°)	Layer separation (Å)	Reference
Two-layer cells							
3D–Cl	Pnma[t]	7·451 (2)	7·200 (2)	18·246 (6)	90	9·123	Phelps et al. (1976)
3D–Br	P2₁/n	8·092	7·563	17·635	96·68	8·758	Halvorson & Willett (1988)
5D–Cl	P2₁/n	7·747 (3)	7·203 (2)	21·769 (6)	102·12 (2)[m]	10·642	This work
5D–Br	P2₁/n	8·142 (3)	7·560 (2)	21·736 (10)	101·49 (3)[m]	10·650	This work
One-layer units							
2D–Cl	P2₁/a	7·158 (3)	7·353 (3)	8·109 (3)	92·37 (3)	8·102	Tichy et al. (1978)
2D–Br	P2₁/a	7·511	7·803	8·334	92·12	8·329	Halvorson & Willett (1988)
3D–Cl	($\frac{1}{2}$ unit)	7·451 (2)	7·200 (2)	9·123 (3)	90	9·123	Phelps et al. (1976)
3D–Br	($\frac{1}{2}$ unit)	8·092	7·563	8·818	96·68	8·758	Halvorson & Willett (1988)
4D–Cl	P2₁/a	7·588 (1)	7·599 (1)	9·268 (1)	103·14 (1)	9·025	This work
4D–Br	P2₁/a	7·914 (2)	7·887 (4)	9·432 (2)	102·83 (2)	9·196	This work
5D–Cl	($\frac{1}{2}$ unit)	7·747 (3)	7·203 (2)	10·884 (3)	102·12 (2)[m]	10·642	This work
5D–Br	($\frac{1}{2}$ unit)	8·1421 (3)	7·560 (2)	10·868 (5)	101·49 (3)[m]	10·650	This work

m = angle of the mirror twin of the crystal studied. t = transformed by exchanging a to b, b to c, and c to a to give a form with layers in the ab plane.

Separate layers are linked *via* the hydrogen-bonded ADA chains. Table 5 summarizes the available data on dihalide bridges expected to be important to the magnetic interaction.

Each N atom is in the position, *gauche* or *trans*, which angles it back most sharply against the monoclinic cell slant. The *gauche* N-atom ends of the 4DA chains have one hydrogen bond to an axial halide and two to halides in the puckered layer. Both *trans* and *gauche* N ends of the 5DA chains have two hydrogen bonds to axial halides and only one to a layer halide. These H-atom positions (not independently located from the X-ray data) are assigned by riding on the N-atom positions. The NH_3 group could be rotated, but the assignments shown in Table 6 give short bond distances to the halides and are consistent with both the bending of the ADA chains and canting of the CuX_4 units. There are some additional H-atom-to-halide distances about 0·5 Å longer which may contribute additional bonding of chains to the layers. A longer discussion (five pages) of the hydrogen-bonding alignments has been deposited.

The orthorhombic 3D–Cl structure occurs with the odd-numbered chain allowing a mirror-symmetry element to pass through the middle C atom of the aliphatic chain. The monoclinic 3D–Br, 5D–Br and

5D–Cl each have one *gauche* end which prevents similar mirror symmetry. Negrier, Couzi, Chanh, Hauw & Meresse (1989) report both orthorhombic and monoclinic forms for 5D–$CdCl_4$ and give phase-transition data. They lack a structure determination for the 5D chains in the monoclinic form but use other information to argue for transition at 337 K from an all-*trans* orthorhombic (similar to 3D–Cl) to orthorhombic partially disordered to 'twisted' chains. Total conversion to 'twisted' chains is proposed at the 417 K transition to monoclinic which reduces the cell volume by about 4%. They argue that thermodynamic data do not fit a carbon chain *trans*-to-*gauche* transition so a less-stable 'twisted' conformation is needed. Their data also fit having one *gauche* N end (like our 5D–Cl and 5D–Br) allowing cell-volume reduction plus disordering of the carbon chain to fit the thermodynamic data. Their observation of the thermodynamically favored all-*trans* orthorhombic form at their lowest T (below 337 K) also suggests our 5D–Cl and 5D–Br might have transitions to orthorhombic if they could form at a low enough temperature.

The (ADA)CuX_4 monoclinic structures show increasing monoclinic slant as the ADA chain lengthens from $n = 2$ to $n = 4$ which lessens the change in interlayer separations. 5D–Cl and 5D–Br have about the same monoclinic angle as the 4DA compounds and a greater change in interlayer separation than seen elsewhere in the series. The 4DA chains are twisted identically at both ends with the N *gauche* to the C_4 chain. That works with the monoclinic slant to shorten the interlayer separation. The end C atoms of the C_4 chain are *trans* around the central C—C bond, so the 4DA chains are *gtg* (*gauche, trans, gauche*) (Halvorson & Willett, 1988). The 5DA chains have dissimilar conformations at the ends of the chain, one *gauche* like the 4DA alignments and one rotated about 90° from that alignment with N *trans* to the C_5 chain. That rotation may account for the similar (not increased) slant and significantly larger layer separation in the

Table 5. *Interlayer halogen–halogen bridging*

	Layer separation (Å)	X—X (Å)	Cu—X—X (°)	Interlayer J'/k	Reference
2D–Cl	8·102	3·649	159·6	−13·7	(a)
3D–Cl	9·123	4·548	171·3	−1·7	(b)
4D–Cl	9·025	4·941	154·8	−0·16	(c)
5D–Cl	10·642	6·525	167·6, 149·6	−0·04	(b)
2D–Br	8·329	3·821	155·7	−68·4	(d)
3D–Br	8·758	4·065	155·8, 171·2	−26	(e)
4D–Br	9·196	4·801	154·9	−5	(e)
5D–Br	10·650	6·234	167·3, 149·2	−2·0	(d)

References: (a) Snively, Seifurt, Emerson & Drumheller (1979); (b) Von Kanel (1979); (c) Snively, Drumheller & Emerson (1981); (d) Rubenacker, Haines, Drumheller & Emerson (1984); (e) Snively, Haines, Emerson & Drumheller (1982).

Table 6. *Hydrogen bonding*

	N—Cl (Å)	C—N—Cl (°)	H—Cl (Å)	N—H—Cl (°)	N—Br (Å)	C—N—Br (°)	H—Br (Å)	N—H—Br (°)
4D–Cl and 4D–Br								
X(1) (layer) on 0,0,0 Cu	3·307	107·4	2·352	173·0	3·444	107·3	2·488	173·4
X(1) on 1,0,0 Cu	3·365	129·5	2·502	149·6	3·520	130·8	2·671	147·6
X(2) (axial) on 0·5, −0·5, 0 Cu	3·204	116·8	2·320	152·8	3·370	115·8	2·476	154·8
5D–Cl and 5D–Br around N(0)								
X(1) (axial) on 0,0,0 Cu	3·273	120·0	2·350	161·1	3·471	122·7	2·573	155·7
X(4) (layer) on 0·5, 0·5, 0 Cu	3·363	87·3	2·512	147·8	3·422	90·0	2·538	153·2
X(2) (axial) on 0·5, −0·5, 0 Cu	3·310	102·0	2·369	165·5	3·663	97·6	2·751	158·9
5D–Cl and 5D–Br around N(6) [with one H fixed along N(6)–X(3) line]								
X(1) (axial) on 0, 0, 0 Cu	3·199	103·2	2·371	144·1	3·526	102·2	2·655	151·1
X(2) (axial) on 0·5, 0·5, 0 Cu	3·277	85·8	2·432	146·7	3·372	90·9	2·505	150·2
X(3) (layer) on 0, 1, 0 Cu	3·412	108·1	2·452	179·7	3·499	103·2	2·534	179·4

5DA structures as compared to the 4DA structures. The C_5 chains in the 5DA structures are all *trans*, making the 5DA unit *tttg*. The *gauche* end is N(0)—C(1)—C(2) in our tables. Adjacent layers in the 2DA and 4DA salts are related by pure translation symmetry, while adjacent layers of the 3DA and 5DA structures are related by glide planes or (for 3*D*–Cl) mirror operations.

5*D*–Br and 5*D*–Cl have about the same ratio of *a/b* and other structural features are very similar. The interlayer dihalide bridge is shorter between the larger Br atoms than between Cl atoms in 5*D*–Cl. This agrees with the antiferromagnetic interlayer J/k being larger for 5*D*–Br than 5*D*–Cl, as reported (Rubenaker, Haines, Drumheller & Emerson, 1984). It does not give any striking structural pattern difference to explain the uncertainty about whether the interlayer coupling in 5*D*–Br is ferromagnetic.

5*D*–Cl and 5*D*–Br have their unique axis, *b*, shortened and the non-unique layer axis, *a*, stretched compared to the 4DA crystals. The monoclinic 3*D*–Br is similar to the 5DA crystals in that pattern for *a versus b*, while the monoclinic 2DA crystals have longer *b* similar to the 4DA crystals. Our choice in Table 4 of the longer axis as *a* for the orthorhombic 3*D*–Cl was based on the angular approach of the chain C—N bond toward the copper halide layer. In the 4DA crystals (where *a* is short) and the 5DA crystals (where *a* is long) the angular deviation of C—N from perpendicular to the layer is greatest in the *a* direction. In 3*D*–Cl that C—N angular deviation from perpendicular is greatest along the 7·451 Å axis we chose as *a*. That makes 3*D*–Cl fit the pattern that odd-carbon-number chains give longer *a* and even-carbon-number chains give shorter *a*. The flexibility of bonding in copper halide sheets is addressed in a paper using a larger selection of examples (Middleton, Place & Willett, 1988).

Differences between the 4DA compounds and the 5DA compounds can be seen in views along the *a* axis shown in Figs. 2 and 3. Fig. 2 shows 4*D*–Br. The middle (4DA) chains (translated by $\frac{1}{2}$**b** and $\frac{1}{2}$**a**) are mirror images (180° different in *b*) of the *b* = 0, or *b* = 1 chains. Fig. 3 shows the comparable view along **a** for 5*D*–Br. The (5DA) chains look like mirror images (180° different in *b*) if the *gauche* N(0) positions are omitted and the C(1) to N(6) *trans* sections are matched. N(6) is mirrored by C(1), C(5) by C(2) and C(4) by C(3).

Fig. 4 shows a view along **b** for 5*D*–Br. The comparable view for 4*D*–Br (Fig. 5) shows seemingly identical chains because the mirror differences in *b* are not seen from that direction. A similar nearly identical matching is seen in Fig. 4 if we omit the *gauche* N(0) positions and match N(6) with C(1), C(5) with C(2), and C(4) with C(3). The N(6)—C(1) pair is not matched as well in Fig. 4 as the

C(5)—C(2) and C(4)—C(3) pairs. The C(1) position varies from matching N(6) in the *a* direction in the manner needed to leave N(0) closer (in *a*) to the center of its 'hole' in the Cu–Br layer. N(0) is unique and C(1) is distorted out of the position mirroring N(6).

4*D*–Cl and 5*D*–Cl are closely similar to the more precisely determined bromides, so we have omitted figures of those structures.
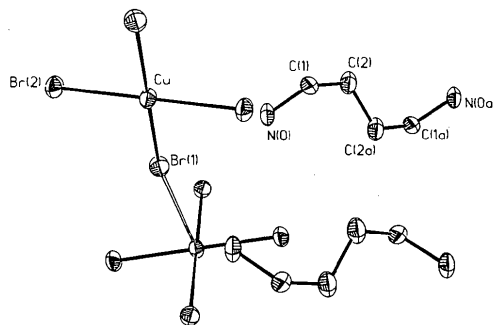

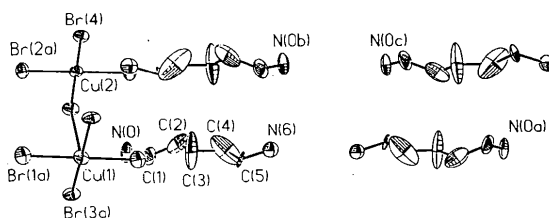
Fig. 2. 4*D*–Br (H atoms omitted) viewed along *a* axis.

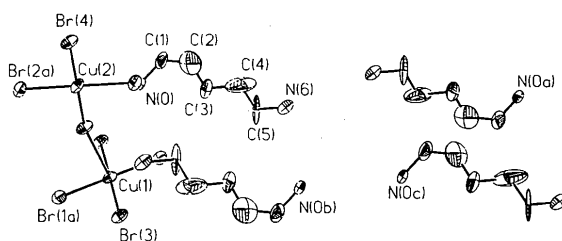
Fig. 3. 5*D*–Br (H atoms omitted) viewed along *a* axis.

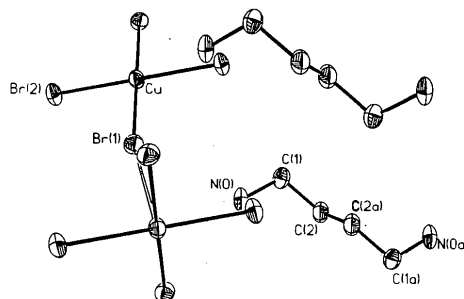
Fig. 4. 5*D*–Br (H atoms omitted) viewed along *b* axis.

Fig. 5. 4*D*–Br (H atoms omitted) viewed along *b* axis.

References

ANDERSON, D. M. & WILLETT, R. D. (1971). *Inorg. Chim. Acta*, **5**, 41–45.

BARENDRECHT, F. & SHENK, H. (1970). *Physica (Utrecht)*, **49**, 465–468.

BIRREL, G. B. & ZASLOW, B. (1972). *J. Inorg. Nucl. Chem.* **34**, 1751.

DRUMHELLER, J. E., DICKEY, D. H., RECKLISS, R. P., ZASPEL, C. E. & GLASS, S. J. (1972). *Phys. Rev. B*, **5**, 4631–4636.

HALVORSON, K. & WILLETT, R. D. (1988). *Acta Cryst.* C44, 2071–2076.

JONGH, L. J. DE & VAN AMSTEL, W. D. (1971). *J. Phys (Paris)*, **32**(C1), 880–881.

JONGH, L. J. DE, VAN AMSTEL, W. D. & MIEDEMA, A. R. (1972). *Physica (Utrecht)*, **58**, 277–304.

MIDDLETON, M., PLACE, H. & WILLETT, R. D. (1988). *J. Am. Chem. Soc.* **110**, 8639–8650.

NEGRIER, P., COUZI, M., CHANH, N. B., HAUW, C. & MERESSE, A. (1989). *J. Phys. (Paris)*, **50**, 405–430.

PHELPS, D. W., LOSEE, D. B., HATFIELD, W. E. & HODGSON, D. J. (1976). *Inorg. Chem.* **15**, 3147–3152.

RUBENACKER, G. V., HAINES, D. N., DRUMHELLER, J. E. & EMERSON, K. (1984). *J. Magn. Magn. Mater.* **43**, 238–242.

SHELDRICK, G. (1984). *SHELXTL Users Manual.* Revision 4.1. Nicolet XRD Corporation, Madison, Wisconsin, USA.

SNIVELY, L. O., DRUMHELLER, J. E. & EMERSON, K. (1981). *Phys. Rev. B*, **23**, 6013–6017.

SNIVELY, L. O., HAINES, D. N., EMERSON, K. & DRUMHELLER, J. E. (1982). *Phys. Rev. B*, **26**, 5245–5247.

SNIVELY, L. O., SEIFURT, P. L., EMERSON, K. & DRUMHELLER, J. E. (1979). *Phys. Rev. B*, **20**, 2101–2104.

SNIVELY, L. O., TUTHILL, G. F. & DRUMHELLER, J. E. (1981). *Phys. Rev. B*, **24**, 5349–5355.

STEADMAN, J. P. & WILLETT, R. D. (1970). *Inorg. Chim. Acta*, **4**, 367–371.

TICHY, K., BENES, J., HAELG, W. & AREND, H. (1978). *Acta Cryst.* B34, 2970–2981.

VON KANEL, H. (1979). *Physica (Utrecht)*, **96B**, 167–193.

WILLETT, R. D. (1964). *J. Chem. Phys.* **41**, 2243–2244.

WONG, R., WILLETT, R. D. & DRUMHELLER, J. E. (1981). *J. Chem. Phys.* **74**, 6018–6021.

ZASPEL, C. E. & DRUMHELLER, J. E. (1977). *Phys. Rev. B*, **16**, 1771–1780.

Structure and Conductivity of Di[3,4;3'4'-bis(ethylenedithio)-2,2',5,5'-tetrathiafulvalenium] Tetrabromomercurate(II)–1,1,2-Trichloroethane, (BEDT-TTF)₂HgBr₄.TCE

BY XIANHUI BU AND PHILIP COPPENS*

Chemistry Department, State University of New York at Buffalo, Buffalo, NY 14214, USA

AND MICHAEL J. NAUGHTON

Department of Physics and Astronomy, State University of New York at Buffalo, Buffalo, NY 14214, USA

Abstract. $[C_{10}H_8S_8]_2[HgBr_4].C_2H_3Cl_3$, $M_r = 1423 \cdot 01$, monoclinic, $C2/c$, $a_A = 56 \cdot 13$ (1), $b_A = 4 \cdot 202$ (1), $c_A = 22 \cdot 306$ (4) Å, $\beta = 100 \cdot 88$ (2)°, $b_B = 2b_A$, where the A lattice represents $C_{10}H_8S_8$, the B lattice the remainder of the atoms, $V_A = 5166$ (3) Å^3, $Z_A = 4$, $D_x = 1 \cdot 83$ g cm^{-3}, λ(Mo $K\alpha$) = 0·71073 Å, $\mu = 68 \cdot 4$ cm^{-1}, $F(000) = 2712$, as summed over the volume of the A cell and including the B atoms of the B lattice, room temperature, $R(F) = 0 \cdot 076$, $wR(F) = 0 \cdot 091$ for 1430 unique reflections. The superlattice layers corresponding to $b_B = 8 \cdot 404$ Å are diffuse indicating short-range ordering of the HgBr₄ structure. The structure consists of sheets of BEDT-TTF cations [BEDT-TTF = bis(ethylenedithio)tetrathiafulvalene]

parallel to the bc plane, separated along the a direction by columns of anions and solvent molecules. Short S—S contacts are found within the cation layers. Tetrahedral HgBr₄ anions form discrete columns with twice the repeat period along the b direction. Four-probe conductivity measurements indicate the solid to be a narrow-band-gap semiconductor.

Introduction. Because of their unusual transport properties salts of BEDT-TTF have attracted considerable attention (Williams *et al.*, 1987). Of particular interest are the organomineral salts, which show the highest superconducting transition temperatures in the BEDT-TTF family or in other organic salts. We report here on the crystal structure

---